

# Performance of Jets and Missing Transverse Energy in ATLAS

---

**Ariel Schwartzman\***

On behalf of the ATLAS Collaboration

SLAC National Accelerator Laboratory

E-mail: [sch@cern.ch](mailto:sch@cern.ch)

After the analysis of the 2010 proton proton collision data provided by LHC, the ATLAS experiment has achieved an accuracy of the jet energy measurement between 2% and 4% for jet transverse momenta from 20 GeV to about 2 TeV in the pseudo-rapidity range up to  $|\eta| = 4.5$ . The jet energy scale uncertainty is derived from in-situ single hadron response measurements along with systematic variations in the Monte Carlo simulation. In addition, several in situ techniques exploiting transverse momentum balance are used. Preliminary results from the 2011 run based on an integrated luminosity of  $5 \text{ fb}^{-1}$  reducing further the uncertainties on the jet energy scale are presented. Results on the energy scale and resolution of the reconstructed missing transverse momentum ( $E_T^{\text{miss}}$ ) from 2010 and 2011 collision data are also presented. The uncertainty evaluation mainly relies on events with a Z-boson. Special attention is given to the influence of the large number of interactions produced in addition to the event of interest (pile-up). Advanced approaches to jet reconstruction using jet grooming algorithms such as filtering, trimming, and pruning are compared. Such techniques aim to reconstruct the jet mass and jet substructure with special focus on highly boosted particles.

*36th International Conference on High Energy Physics,  
July 4-11, 2012  
Melbourne, Australia*

---

\*Speaker.



## 1. Introduction

Jets are among the main ingredients in most physics analyses at the LHC. During the last several years, many new ideas for the analysis and interpretation of hadronic final states at the LHC have been proposed by the theory community, and rapidly implemented and commissioned by the ATLAS experiment. At the same time, LHC's unprecedented high luminosity environment has introduced difficult challenges for the reconstruction and calibration of jets and  $E_T^{\text{miss}}$ . The excellent ATLAS detector capabilities, in particular its high resolution longitudinally segmented calorimeter and inner detector, as well as an accurate detector simulation, have enabled the development of complex clustering and calibration algorithms for the reconstruction of jets,  $E_T^{\text{miss}}$  and jet substructure. The high integrated luminosity provided by the LHC during 2011 has also allowed the use of large calibration datasets to significantly reduce the jet energy scale uncertainty.

## 2. Jet reconstruction and calibration

The input to jet reconstruction in ATLAS are locally-calibrated three-dimensional *topological clusters* (topoclusters), build from calorimeter cells. Topoclustering starts by identifying seed cells with energy significance above  $4\sigma$  noise, where the noise is defined as the sum in quadrature of electronic and pile-up noise. The noise threshold used for jet and  $E_T^{\text{miss}}$  reconstruction in 2011 was equivalent to the average cell energy in events with 8 additional interactions. Neighbor cells with energy significance higher than two are then iteratively added to seed clusters. An extra layer of direct neighbor cells is added to the final clusters. After topoclusters are found, a splitting algorithm further separates clusters based on local energy maxima within clusters. Individual clusters are calibrated using local properties such as energy density, calorimeter depth, and isolation with respect to nearby clusters. This local cluster weighting calibration (LCW) allows to classify clusters as electromagnetic or hadronic and uses a dedicated cluster calibration derived from single pion Monte Carlo simulations. Such calibration significantly improves the constant term of the jet energy resolution, reduces the flavor dependence of the jet response, and facilitates the implementation of jet substructure techniques by providing calibrated constituents as inputs to jet reconstruction.

Jets are built using the anti- $k_r$  algorithm [1] with radius parameters  $R=0.4$  and  $R=0.6$ . Additionally, ATLAS now provides several *large-R* jet algorithms such as anti- $k_r$  jets with  $R = 1.0$  and Cambridge-Aachen (C/A) jets with  $R = 1.2$  using trimming [2], pruning [3], and filtering [4].

Jets are calibrated to particle level in QCD events using a multistep, sequential scheme, consisting of i) a Monte Carlo pile-up offset correction, ii) a Monte Carlo jet energy response correction, and iii) an in situ residual calibration applied to jets in data only, to account for the differences in response between data and Monte Carlo. Optional, post-calibration jet-by-jet corrections are available, in particular some using tracking information.

### 2.1 Pile-up subtraction and suppression

Additional pp interactions originated by the same bunch crossing add extra energy (offset) to jets that need to be subtracted. Furthermore, pile-up fluctuations increase the noise term of

the jet energy resolution and can create additional (fake) jets that need to be suppressed. The pile-up jet offset correction accounts for the effect of both in-time and out-of-time pile-up. In-time pile-up refers to the extra interactions produced within an event. Out-of-time pile-up is due to the cumulative effect of energy depositions before and after the triggered event, due to the large integration time (400-600 ns) of the calorimeter relative to the bunch spacing (50 ns). The offset correction is determined from Monte Carlo, and parametrized as an average jet  $p_T$  subtraction as a function of the number of primary vertices and the instantaneous luminosity of a given event. The offset uncertainty is obtained from the differences between Monte Carlo and in situ measurements of the jet offset using  $\gamma$ +jet and dijet events.

Additional fake jets originating from pile-up fluctuations after the application of the offset correction are rejected using the Jet Vertex Fraction (JVF) algorithm. JVF calculates the fraction of total track  $p_T$  matched to a jet that originates from the hard scatter vertex. Pile-up jets have very small JVF values as most of their tracks originate from additional pile-up vertices.

## 2.2 Jet energy scale uncertainty

In 2010, the jet energy scale uncertainty was determined using a combination of single pion test beam and in situ pp measurements and Monte Carlo samples generated with different detector configurations and physics models with respect to the nominal Pythia [5] Monte Carlo sample used to derive the jet energy scale. The total uncertainty was smaller than 2.5% for central jets with  $p_T > 100$  GeV, and smaller than 7% (14%) for jets in the endcap (forward) calorimeter regions.

In 2011, large samples of dijet, Z+jet, and  $\gamma$ +jet events have enabled in situ measurements of the jet response with better precision than what was previously obtained with Monte Carlo methods.

Two techniques were used to establish the jet energy scale in  $\gamma$ +jet events. The direct  $\gamma$ +jet balance method, and the missing  $p_T$  fraction method (MPF). In the direct  $\gamma$ +jet balance technique, the balance between the photon and the leading jet is measured. The MPF technique considers the balance between the photon and the full hadronic recoil in the event, given by the projection of the missing transverse energy into the direction of the photon. Both measurements lead to a total jet energy scale uncertainty smaller than 1% for jets with  $100 < p_T < 500$  GeV. Figure 1 shows the data to Monte Carlo ratio of the MPF response and the sources of uncertainties, as a function of the photon  $p_T$ .

The Z+jet balance technique probes the jet response at low jet  $p_T$  due to the use of low  $p_T$  threshold triggers and the smaller backgrounds compared to  $\gamma$ +jet events. Figure 2 (a) shows the double ratio of the  $p_T$  balance between the leading jet and the Z-boson (reference object) in data and Monte Carlo, as a function of the Z-boson  $p_T$  [6]. The uncertainty from this measurement is between 1% and 2% for jets with  $p_T > 30$  GeV.

## 2.3 Jet energy resolution improvement using tracks

Tracking information is incorporated after jet reconstruction and calibration to refine the jet energy scale, jet-by-jet, leading to an improved jet performance by reducing some sources of fluctuations. A track-multiplicity correction, derived from Monte Carlo, corrects the jet energy response depending on the number of charged particles matched to the jet. Tracks originating from the primary vertex with  $p_T > 1$  GeV are considered. The correction works such that jets with large

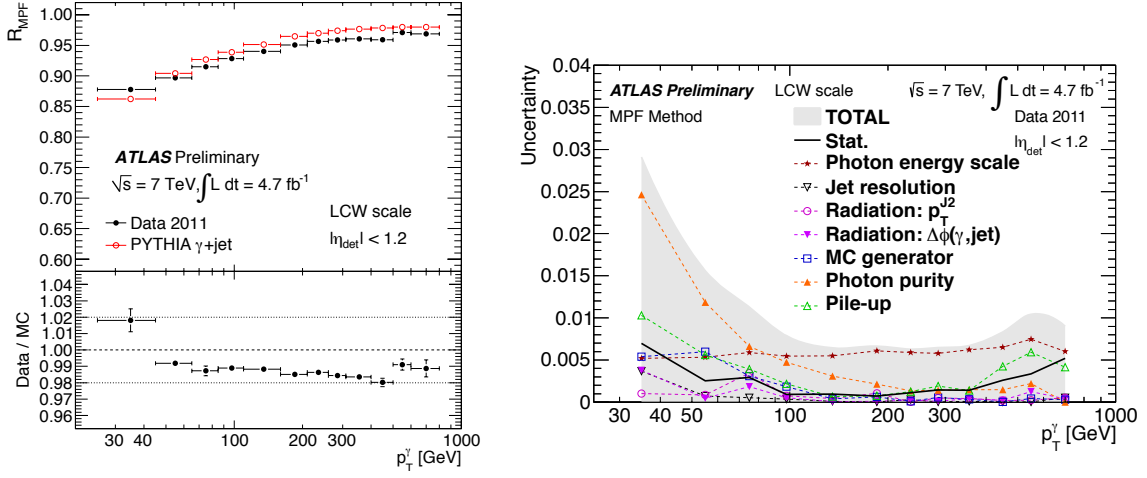


**Figure 1:** (a) Average jet response as determined by the MPF technique using topoclusters at LCW energy scale, for both data and MC, as a function of the photon transverse momentum. The data-to-MC response ratio is shown in the bottom inset of the figure [7]. Only the statistical uncertainties are shown. (b) Systematic uncertainties on the ratio of the jet response in data over MC as determined by the MPF technique using topoclusters at the LCW energy scale, as a function of the photon transverse momentum [7].

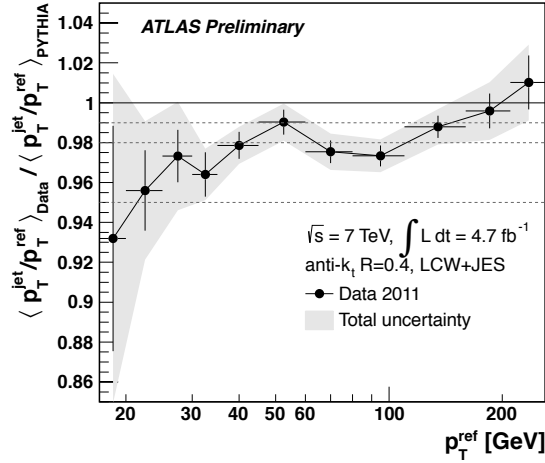


**Figure 2:** Data-to-MC ratio of the mean  $p_T$  balance as a function of the  $p_T$  of the Z-boson ( $p_T^{ref}$ ) for anti- $k_t$  jets with radius parameter  $R=0.4$  calibrated with the LCW scheme. The total uncertainty on this ratio is depicted by gray bands. Dashed lines show the -1%, -2%, and -5% shifts [6].

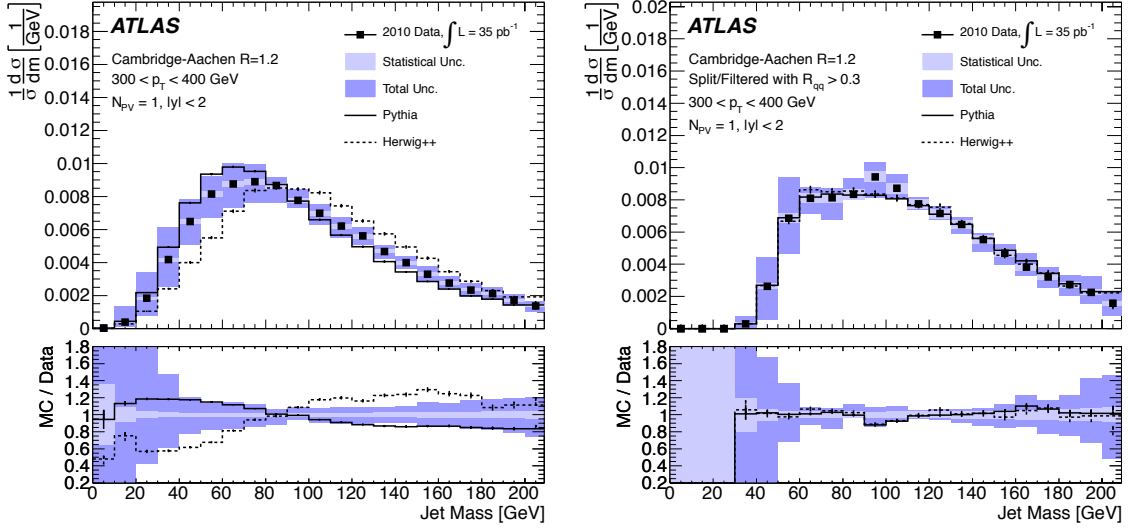


**Figure 3:** Normalised cross-section as a function of mass of Cambridge-Aachen jets with  $R = 1.2$  before (a) and after (b) splitting and filtering [9]

number of tracks receive a higher correction than jets with smaller track multiplicity. No one-to-one matching between tracks and calorimeter clusters is required in this technique. This method improves the jet energy resolution of  $R=0.4$  anti- $k_t$  jets by 10% for jets with  $p_T < 200$  GeV, and significantly reduces the flavor dependence of the jet response (response differences between quark- and gluon-initiated jets)

### 3. Jet mass and jet substructure

ATLAS has commissioned several new powerful tools for the identification of boosted heavy particles. These techniques attempt to distinguish jets from the decay of massive objects from QCD jets with similar masses. Grooming algorithms, in particular, have been shown to improve the jet mass resolution, increase signal over background, and significantly reduce the effects of pile-up on the jet mass.

A key element to enable the use of these techniques for physics measurements is the study of the internal structure of jets generated by QCD radiation. ATLAS has tested inclusive samples of jets recorded with the detector in 2010, which corresponds to  $35 \text{ pb}^{-1}$  of pp collisions delivered by the LHC at  $\sqrt{s} = 7$  TeV.

Figure 3 shows the jet mass distribution in data for Cambridge-Aachen jets with  $R = 1.2$  before and after the splitting and filtering grooming algorithm [4].

There is broad agreement between data and leading-order parton-shower Monte Carlo predictions from Pythia [5] and Herwig++ [8] however, the jet mass after the Cambridge-Aachen splitting and filtering procedure shows a very good agreement with both Monte Carlo simulations. Similar results have been obtained for several other jet substructure observable such as  $k_t$  splitting scales and  $n$ -subjettiness [9], indicating that jet mass and substructure quantities can be successfully reproduced by leading-order parton-shower Monte Carlo generators.

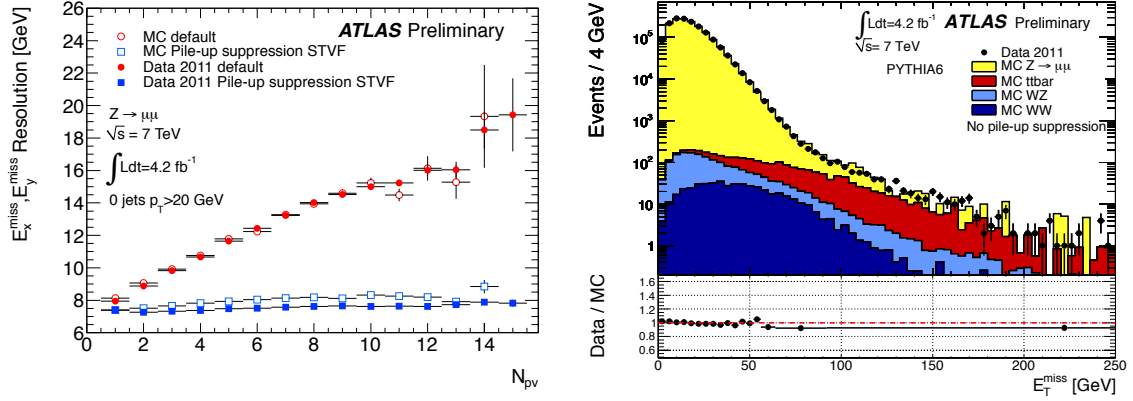


**Figure 4:** (a)  $E_T^{\text{miss}}$  resolution as a function of the number of primary vertices in  $Z \rightarrow \mu\mu$  events without jets with  $p_T > 20$  GeV. The default  $E_T^{\text{miss}}$  is compared with the  $E_T^{\text{miss}}$  after the pile-up correction using the soft term vertex fraction [10]. (b) Distribution of  $E_T^{\text{miss}}$  as measured in a data sample of  $Z \rightarrow \mu\mu$  events. The expectation from Monte Carlo simulation (Pythia 6) is superimposed and normalized to data, after each MC sample is weighted with its corresponding cross-section. The lower part of the figures show the ratio of data over Monte Carlo [10]

#### 4. Missing Transverse energy performance

The  $E_T^{\text{miss}}$  is reconstructed from cells belonging to topoclusters and from reconstructed muons. Cells in topoclusters are calibrated using the LCW calibration described in section 2. The calibration of all physics objects in each final state is also propagated to the  $E_T^{\text{miss}}$ . The *soft term* of the missing ET, which consists of topoclusters not belonging to any reconstructed physics object, is corrected for the effect of pile-up using a track-based technique. The Soft Term Vertex Fraction (STVF) is defined as the ratio of all tracks unmatched to jets from the hard-scatter vertex and all tracks unmatched to jets from all vertices in a given event. The soft term of the  $E_T^{\text{miss}}$  is then rescaled by STVF, event-by-event. Figure 4 (a) shows the resolution of the  $E_T^{\text{miss}}$  in  $Z \rightarrow \mu\mu$  events as a function of the number of primary vertices before and after the STVF pile-up suppression, in data and Monte Carlo. In events with no jets in the final state, the STVF pile-up suppression algorithm restores the  $E_T^{\text{miss}}$  resolution to the corresponding resolution in events without pile-up, and makes the  $E_T^{\text{miss}}$  resolution independent of the number of additional interactions.

The  $E_T^{\text{miss}}$  performance and systematic uncertainties are established from differences between data and Monte Carlo of the  $E_T^{\text{miss}}$  distribution in  $Z \rightarrow ll$  and  $W \rightarrow e\nu$  events, as shown in Figure 4 (b) for the case of  $Z \rightarrow ll$  events.

#### 5. Conclusions

ATLAS has achieved a very high precision on the jet and missing transverse energy performance by the use of sophisticated topological clustering and local cluster calibration, pile-up subtraction methods, and in situ techniques to correct for the residual jet energy response difference between data and simulation. Tracking information is being combined with calorimeter information to further improve the jet and missing ET performance. ATLAS has also commissioned

jet mass, jet substructure, and several new jet algorithms as powerful tools to enhance the LHC physics potential for boosted signatures.

## References

- [1] M. Cacciari, G. P. Salam, and G. Soyez, *The anti-kt jet clustering algorithm*, *JHEP* **04** (2008) 063, [arXiv:0802.1189].
- [2] D. Krohn, J. Thaler, and L.-T. Wang, *Jet trimming*, *JHEP* **2010** (2010) 20, [arXiv:0912.1342]
- [3] S. D. Ellis, C. K. Vermilion, and J. R. Walsh, *Recombination Algorithms and Jet Substructure: Pruning as a Tool for Heavy Particle Searches*, *Phys. Rev.* **D81** (2010) 094023, arXiv:0912.0033 [hep-ph].
- [4] J. M. Butterworth, A. R. Davison, M. Rubin, and G. P. Salam, *Jet substructure as a new Higgs search channel at the LHC*, *Phys. Rev. Lett.* **100** (2008) 242001, [arXiv:0802.2470].
- [5] T. Sjostrand, S. Mrenna, and P. Skands, *PYTHIA 6.4 physics and manual*, *JHEP* **05** (2006) 026, [arXiv:hep-ph/0603175].
- [6] ATLAS Collaboration, *Probing the measurement of jet energies with the ATLAS detector using Z+jet events from proton-proton collisions at  $\sqrt{s} = 7\text{TeV}$* , ATLAS-CONF-2012-053.
- [7] ATLAS Collaboration, *Probing the measurement of jet energies with the ATLAS detector using photon+jet events in proton-proton collisions at  $\sqrt{s} = 7\text{TeV}$* , ATLAS-CONF-2012-063.
- [8] M. Bahr et. al., *Herwig++ physics and manual*, *Eur. Phys. J. C* **58** (2008) 639-707, [arXiv:0803.0883].
- [9] ATLAS Collaboration, *Jet mass and substructure of inclusive jets in  $\sqrt{s} = 7\text{TeV}$  pp collisions with the ATLAS experiment*, *JHEP* **1205** (2012) 128.
- [10] ATLAS Collaboration, *Reconstruction and Calibration of Missing Transverse Energy and Performance in Z and W events in ATLAS Proton-Proton Collisions at  $\sqrt{s} = 7\text{TeV}$* , ATLAS-CONF-2012-101.